Conflicting Physiological and Genomic Cardiopulmonary Effects of Recruitment Maneuvers in Murine Acute Lung Injury

Armand Mekontso Dessap[1,2,3]*, Guillaume Voiriot[1,2]*, Tong Zhou[4], Elisabeth Marcos[1,2], Steven M. Dudek[4], Jeff R. Jacobson[4], Roberto Machado[4], Serge Adnot[1,2], Laurent Brochard[5], Bernard Maitre[1,2,3], and Joe G. N. Garcia[4]

[1]INSERM, Unité U955 (Institut Mondor de Recherche Biomédicale), Créteil, France; [2]Université Paris Est Créteil Val de Marne, Faculté de Médecine, Créteil, France; [3]AP-HP, Groupe Henri Mondor–Albert Chenevier, Service de Réanimation Médicale, Créteil, France; [4]Institute for Personalized Respiratory Medicine, Section of Pulmonary, Critical Care, Sleep and Allergy, University of Illinois at Chicago, Chicago, Illinois; and [5]Intensive Care Unit, Geneva University Hospital, and Geneva University, Geneva, Switzerland

Low tidal volume ventilation, although promoting atelectasis, is a protective strategy against ventilator-induced lung injury. Deep inflation (DI) recruitment maneuvers restore lung volumes, but potentially compromise lung parenchymal and vascular function via repetitive overdistention. Our objective was to examine cardiopulmonary physiological and transcriptional consequences of recruitment maneuvers. C57/BL6 mice challenged with either PBS or LPS via aspiration were placed on mechanical ventilation (5 h) using low tidal volume inflation (TI; 8 μl/g) alone or in combination with intermittent DIs (0.75 ml twice/min). Lung mechanics during TI ventilation significantly deteriorated, as assessed by forced oscillation technique and pressure–volume curves. DI mitigated the TI-induced alterations in lung mechanics, but induced a significant rise in right ventricle systolic pressures and pulmonary vascular resistances, especially in LPS-challenged animals. In addition, DI exacerbated the LPS-induced genome-wide lung inflammatory transcriptome, with prominent dysregulation of a gene cluster involving vascular processes, as well as increases in cytokine concentrations in bronchoalveolar lavage fluid and plasma. Gene ontology analyses of right ventricular tissue expression profiles also identified inflammatory signatures, as well as apoptosis and membrane organization ontologies, as potential elements in the response to acute pressure overload. Our results, although confirming the improvement in lung mechanics offered by DI, highlight a detrimental impact in sustaining inflammatory response and exacerbating lung vascular dysfunction, events contributing to increases in right ventricle afterload. These novel insights should be integrated into the clinical assessment of the risk/benefit of recruitment maneuver strategies.

Keywords: mechanical ventilation; microarray; pulmonary hypertension; right ventricle; acute lung injury

Studies demonstrating lower mortality rates in patients with acute lung injury (ALI) and acute respiratory distress syndrome (ARDS) receiving low tidal volume ventilation (1, 2) have resulted in adoption of these ventilation guidelines in clinical practice (3). However, low tidal volume ventilation also promotes atelectasis (4), with the potential to worsen lung injury through local alveolar hypoxia, increases in lung permeability (5), and lung inflammation (6). Local intrapulmonary shear forces generated during repeated reopening of atelectatic alveoli may also accelerate injury (7). Deep inflation (DI) recruitment maneuvers have been proposed as a means of periodically reopening regions of atelectasis. Experimental and clinical studies have demonstrated improvement in oxygenation, ventilation, and lung mechanical function after DI, without evidence of lung injury (8, 9). However, several adverse cardiovascular effects have been noted with lung recruitment maneuvers, with both high intrathoracic pressures (potentially leading to a decrease in systemic venous return) and high transpulmonary pressures (with the potential for increases in right ventricular afterload via compression and stretch of small alveolar vessels) (10–12). Although preload effects may be easily mitigated by fluid loading (12), DI-induced afterload effects may prompt right ventricular compromise (13, 14).

As pulmonary vascular dysfunction has been recognized as common during ALI and independently associated with poor outcomes (15), the aim of the present work was to examine the physiological and genomic effects of DI on lung mechanics and right ventricle function. Using a murine model of lung injury with prolonged low tidal volume mechanical ventilation, we assessed physiological and genomic cardiopulmonary responses to DI and performed multianalyte profiling of cytokines, chemokines, and markers of endothelial injury in plasma and bronchoalveolar lavage (BAL) fluid. Some of the results of this study have been previously reported in the form of an abstract (16).

MATERIALS AND METHODS

Additional details on the methods are provided in the online supplement.

Animal Protocol

Male C57BL/6 mice, weighing 20–30 g, were anesthetized with inhaled 5% isoflurane (Abbott, Rungis, France), and aspirated a 50-μl volume instillate (consisting of PBS or 4 μg/g of *Escherichia coli* LPS, O55:B5; Sigma-Aldrich, Chimie, Lyon, France) into the lower respiratory tract (17). After oropharyngeal aspiration, the mice were returned to their cages for 18 hours, then were reanesthetized and intubated for mechanical ventilation (*see* online supplement for details).

Mechanical Ventilation

Mice were ventilated in the supine position using humidified gas, by means of a computer-driven small-animal ventilator (flexiVent; Scireq, Montreal, PQ, Canada) as follows: tidal volume, 8 μl/g of body weight; respiratory rate, 180/min; end-expiratory pressure, 3 cm H_2O; and $F_{I_{O_2}}$, 1 (18). Mechanical ventilation lasted 5 hours with continuous anesthesia,

(*Received in original form August 31, 2011 and in final form November 16, 2011*)

* A.M.D. and G.V. contributed equally to this work.

This work was supported by grants from the Monahan foundation (A.M.D.), Société de Réanimation de Langue Française (AMD), Société Française d'Anesthésie Réanimation (A.M.D.), Laboratoires Servier (A.M.D.), and National Institutes of Health grant HL58094 (J.G.N.G.).

Correspondence and requests for reprints should be addressed to Joe G. N. Garcia, M.D., Vice Chancellor for Research, University of Illinois at Chicago, 1737 West Polk Street, 305D AOB, Chicago, IL 60612-7227. E-mail: jggarcia@uic.edu

This article has an online supplement, which is accessible from this issue's table of contents at www.atsjournals.org

Am J Respir Cell Mol Biol Vol 46, Iss. 4, pp 541–550, Apr 2012

Originally Published in Press as DOI: 10.1165/rcmb.2011-0306OC on December 1, 2011
Internet address: www.atsjournals.org

muscle paralysis, a body temperature maintained at 36.5°C, and regular intraperitoneal warm fluid boluses (*see* online supplement for details).

Experimental Design

The experimental design included four groups: PBS + TI (PBS aspiration followed by mechanical ventilation with tidal inflations only); PBS + DI (PBS aspiration followed by mechanical ventilation with intermittent DI); LPS + TI (LPS aspiration followed by mechanical ventilation with tidal inflations only); and LPS + DI (LPS aspiration followed by mechanical ventilation with intermittent DI). DI maneuvers were supplied by the flexiVent ventilator (*see* online supplement for details) as a volume of 0.75 ml delivered twice per minute, as this recruitment strategy was previously shown to safely improve lung mechanics during a 2-hour ventilation protocol in a murine model while conferring protection from biotrauma (8).

Respiratory Mechanics

Forced oscillation techniques (FOTs) were assessed at initiation of mechanical ventilation (before and after volume history standardization), and then repeated hourly, for calculation of respiratory system dynamic resistance, elastance, and compliance (single-frequency FOT data), as well as airway Newtonian resistance, tissue damping, and tissue elastance (low-frequency FOT data) (19, 20). In addition, quasistatic compliance of the respiratory system was evaluated from a continuous pressure–volume curve performed at start and end of mechanical ventilation (*see* online supplement for details).

Hemodynamic Explorations

Before the end of the timed ventilator protocol, mice underwent hemodynamic explorations. Right ventricular systolic pressure was measured during a short respiratory pause via jugular catheterization with an ultraminiature 1.4 F high-fidelity pressure transducer catheter, and cardiac output was measured by the transpulmonary thermodilution technique (21) (*see* online supplement for details). Total pulmonary vascular resistances were calculated as the ratio of right ventricular systolic pressure to cardiac output.

Specimen Collection

After hemodynamic measurements, arterial blood was obtained via carotid puncture for determination of blood gases and subsequent

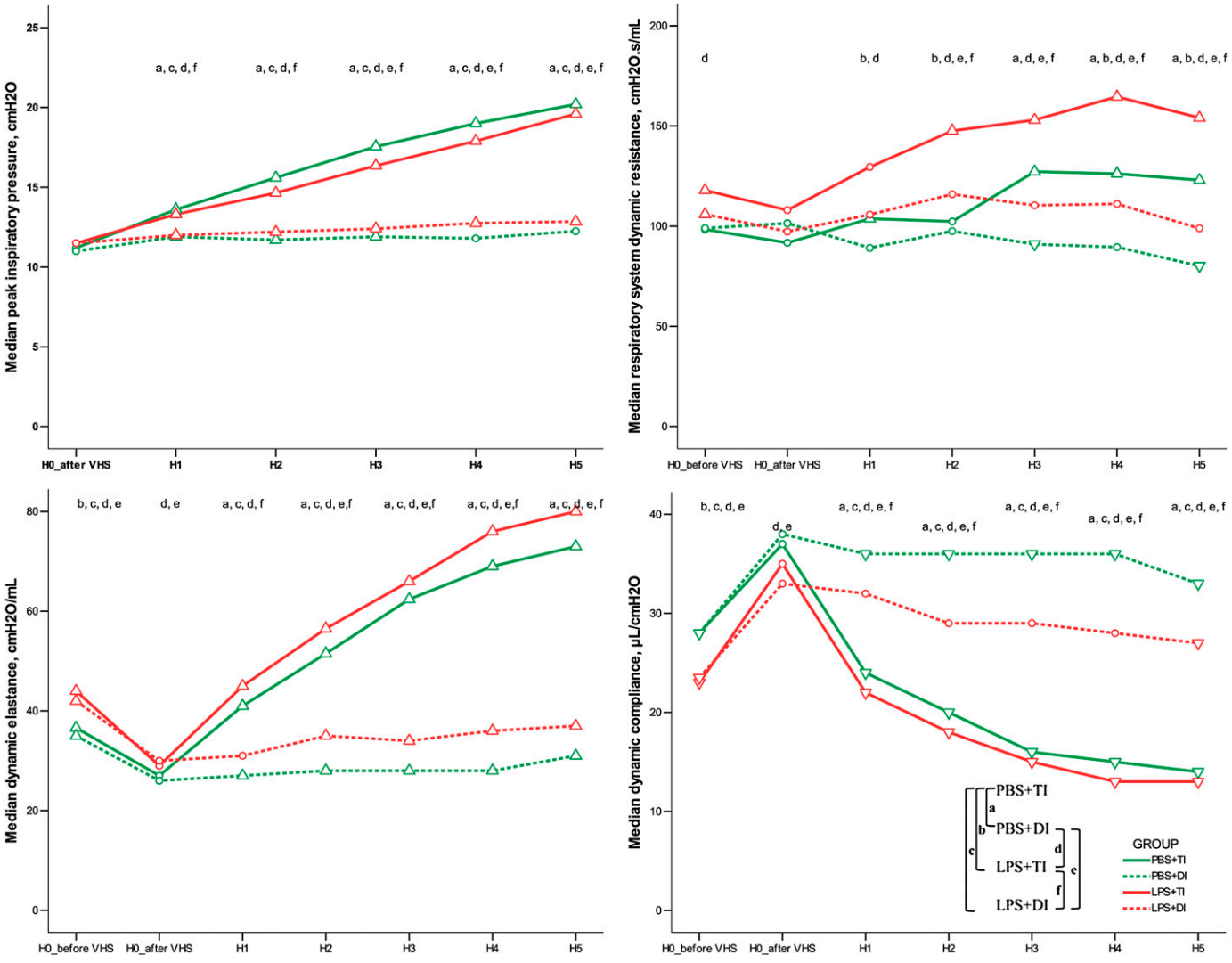

Figure 1. Airway pressures monitoring and single-frequency forced oscillation technique (FOT) results during 5 hours of mechanical ventilation using tidal inflations (TIs) or deep inflations (DIs) in mice after PBS or LPS aspiration. The depicted nomenclature of a, b, c, d, e, and f denote a Bonferroni-corrected *P* value less than 0.05 for the Mann-Whitney pairwise comparisons (after Kruskal Wallis test): PBS + TI versus PBS + DI, PBS + TI versus LPS + TI, PBS + TI versus LPS + DI, PBS + DI versus LPS + TI, PBS + DI versus LPD + DI, and LPS + TI versus LPS + DI, respectively. *Triangles* and *inverted triangles* denote significant increase and decrease, respectively (as compared with H0_after volume history standardization) with Bonferroni-corrected *P* value less than 0.05 for pairwise Wilcoxon (after Friedman's test) ($n = 6$–9 animals per group). H0_before VHS denotes experiment start before volume history standardization. H0_after VHS denotes experiment start after volume history standardization.

measurement of cytokines, chemokines, and markers of endothelial injury using mouse multianalyte cytokine kits (*see* online supplement for details). Cardiac right and left ventricles, as well as right lower lobe of the lung, were harvested, quick frozen in liquid nitrogen, and stored at −80°C (*see* online supplement for details). The remaining lung was lavaged with four separate 0.5-ml aliquots of saline at 20°C and underwent fixation (4% paraformaldehyde) and paraffin embedding.

BAL

The total cell count was determined for a fresh fluid specimen using a Malassez hemocytometer. BAL fluid was centrifuged (1,600 rpm, 7 min, 4°C), and cell-free supernatants were stored at −80°C for subsequent assessment of protein content and multianalyte cytokine and chemokine concentrations (*see* online supplement for details).

Histological Analysis

Lung sections of 5-μm thickness were cut and stained with hematoxylin and eosin. True-color, high-resolution digital images were obtained from stained slides using an Aperio ScanScope CS scanner (Aperio, Vista, CA) with a 20× scanning magnification. The degree of lung edema and vascular congestion were blindly determined using a high-speed automated whole-slide quantitative image analysis tool (Genie histology pattern recognition, ImageScope version 6.25 software; Aperio) (*see* online supplement for details) (22).

RNA Isolation and Transcript Analysis

We extracted total RNA from frozen tissues (three to four animals per group) with a combined protocol using TRIzol reagent (Invitrogen, Carlsbad, CA) and the RNeasy kit (Qiagen, Valencia, CA), as previously described (23, 24). We used total RNA (5 μg) to synthesize double-stranded cDNA, then biotin-labeled antisense cRNA which was fragmented and hybridized to the Affymetrix Mouse Genome 430 2.0 Array (containing ~34,000 genes; Affymetrix, Santa Clara, CA) (*see* online supplement for details).

Oligonucleotide Array Analysis

After quality evaluation (25, 26), arrays were normalized and processed using the Bioconductor "GCRMA" package (http://www.bioconductor.org). To identify differentially expressed genes, we conducted pairwise

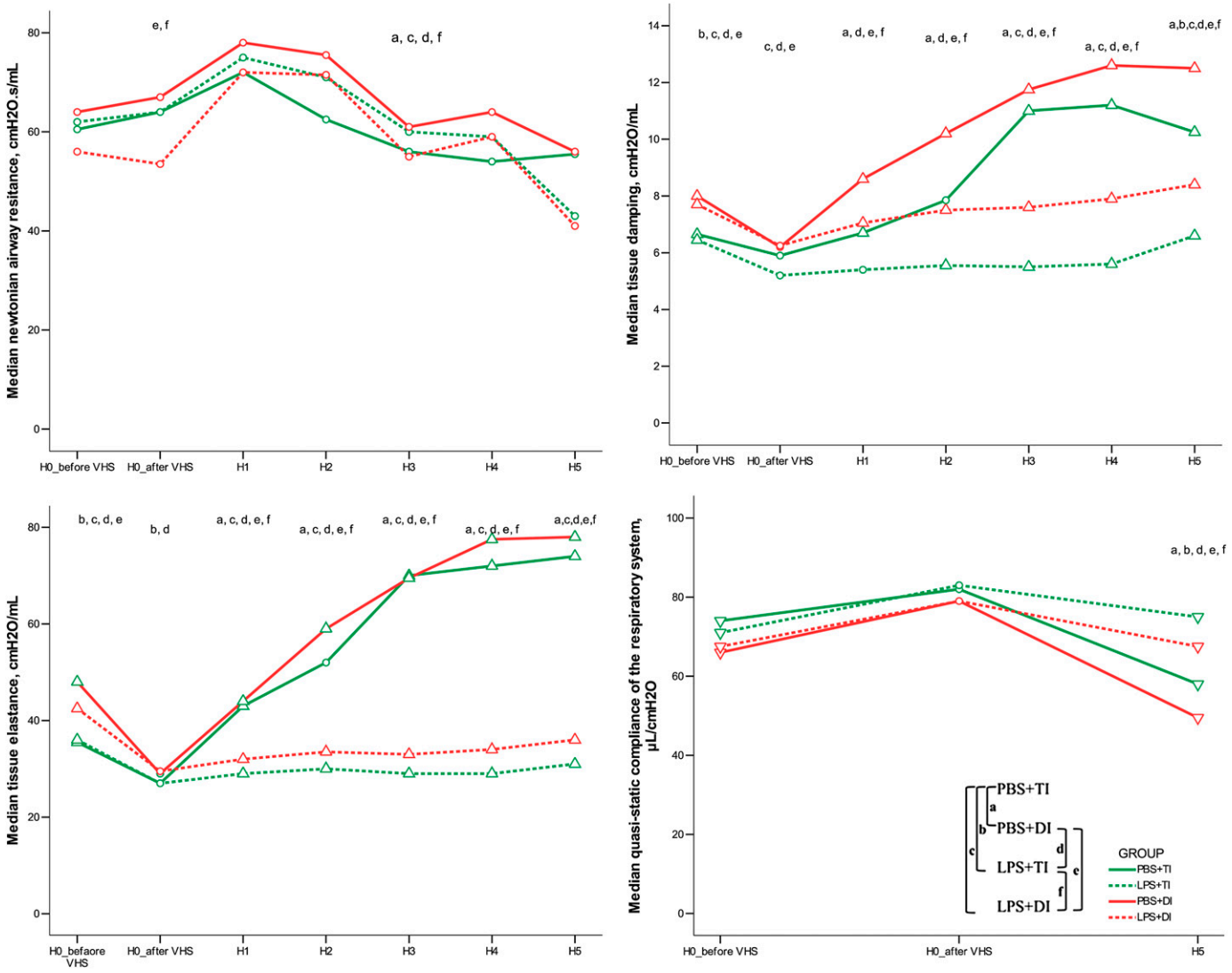

Figure 2. Low-frequency FOT results and pressure–volume curve data before and during 5 hours of mechanical ventilation using TIs or DIs in mice after PBS or LPS aspiration. a, b, c, d, e, and f denote a Bonferroni-corrected *P* value less than 0.05 for the Mann-Whitney pairwise comparisons (after Kruskal Wallis test): PBS + TI versus PBS + DI, PBS + TI versus LPS + TI, PBS + TI versus LPS + DI, PBS + DI versus LPS + TI, PBS + DI versus LPD + DI, and LPS + TI versus LPS + DI, respectively. *Triangles* and *inverted triangles* denote significant increase and decrease, respectively (as compared with H0_after volume history standardization) with Bonferroni-corrected *P* value less than 0.05 for pairwise Wilcoxon (after Friedman's test) ($n = 6$–9 animals per group). H0_before VHS denotes experiment start before volume history standardization. H0_after VHS denotes experiment start after volume history standardization.

comparisons using Significance Analysis of Microarrays (27) (*see* online supplement for details).

Identification of Gene Ontology Categories and Pathways Enriched with Dysregulated Genes

The lists of dysregulated genes were imported into Database for Annotation, Visualization and Integrated Discovery (DAVID; http://david.abcc.ncifcrf.gov/) (28). The genes in these lists were mapped to DAVID identifiers, and then functionally annotated using the DAVID default gene ontology categories and pathways (*see* online supplement for details).

Quantitative RT-PCR

Quantification of selected transcripts was performed by TaqMan real-time RT-PCR assays using a CFX384 Rea-Time PCR Detection System (Bio-Rad, Hercules, CA) (*see* online supplement for details).

Statistical Analysis of Nonmicroarray Data

The data were analyzed using the SPSS Base 13.0 statistical software package (SPSS Inc., Chicago, IL). Continuous data were expressed as median (first through third quartiles), unless otherwise stated. Independent samples were compared using the Kruskal-Wallis test followed by pairwise Mann-Whitney test. Related samples were compared using the Friedman test followed by pairwise Wilcoxon test (with Bonferroni correction). Categorical variables, expressed as percentages, were evaluated using the chi-square test or Fisher exact test. Two-tailed P values smaller than 0.05 were considered significant.

RESULTS

Effect of DI on Respiratory and Hemodynamic Parameters

Results of respiratory monitoring, FOT, and pressure–volume curves are displayed in Figures 1 and 2. Manual adjustment for a delivered tidal volume of 8 μl/g of body weight resulted in a constant minute ventilation throughout the experiment in all groups. At initiation of mechanical ventilation, animals challenged with LPS exhibited higher values of dynamic elastance, tissue damping, and tissue elastance as compared with those having received PBS. This difference partially persisted after volume history standardization and during mechanical ventilation. Mechanical ventilation with TI was associated with a progressive and major increase in airway pressures, dynamic elastance, tissue damping, and tissue elastance, whereas dynamic compliance and quasistatic compliance decreased, with each change significantly mitigated in groups receiving DI. Arterial blood gas analysis, BAL data, and quantitative histological assessment at the end of the ventilation protocol are reported in Table 1. LPS challenge was associated with an increase in BAL fluid cell count, as well as histological evidence of increased lung edema and vascular congestion.

Hemodynamic data at the end of the ventilation protocol are reported in Table 2, with heart rates and cardiac outputs comparable among groups. Right ventricular systolic pressure and total pulmonary vascular resistances were increased in all groups as compared with the PBS + TI group, with the highest values observed in the LPS + DI group.

Effect of DI on Genomic Parameters

The gene-filtering parameters of significance analysis of microarray and the number of dysregulated genes in lung and heart tissues identified by pairwise comparisons (PBS + TI as reference group) are summarized in Table E1 in the online supplement. Lung gene expression profiling showed robust differential expression for both LPS + TI (660 genes) and LPS + DI (1,697 genes). Gene expression profiles were not significantly different between PBS + DI group and the PBS + TI reference group, suggesting the absence of prominent effects of DI in the absence of lung injury. Clustered heat maps revealed that most dysregulated lung genes from LPS + TI animals were also dysregulated in LPS + DI animals (Figure 3), with gene ontology and pathway functional annotation clustering revealing significant overlap. Among the top 10 common enriched clusters were clusters involving inflammatory responses, chemotaxis, cell migration, microsomes, extracellular matrix, and carbohydrate binding (Figure 4). Interestingly, a unique dysregulated cluster significantly enriched in LPS + DI lungs (rank 3), but not by LPS + TI involved genes related to vascular processes (Figure 4 and Figure E1). For example, genes involved in the vascular smooth muscle contraction pathway were significantly dysregulated in LPS + DI lungs, but not by LPS + TI (Figure E2). The fold change levels in gene expression for selected, significantly dysregulated genes by LPS + DI involved in lung inflammation and lung vascular dysfunction (endothelial injury, microvascular thrombosis, vascular tone and remodeling) are displayed in Figure 5A. Genome-wide expression profiling results

TABLE 1. ARTERIAL BLOOD GASES, BRONCHOALVEOLAR LAVAGE DATA, AND HISTOLOGICAL ANALYSIS AT THE END OF 5 HOURS OF MECHANICAL VENTILATION USING TIDAL INFLATIONS OR DEEP INFLATIONS IN MICE THAT UNDERWENT PBS OR LPS ASPIRATION

	PBS + TI	PBS + DI	LPS + TI	LPS + DI
Arterial blood gases				
Pa_{O_2}/FI_{O_2}	289 (270–394)	306 (265–339)	268 (205–296)	283 (274–339)
pH	7.19 (7.15–7.30)	7.34 (7.29–7.41)*	7.17 (7.07–7.22)†	7.24 (7.16–7.32)
Pa_{CO_2}, mm Hg	34 (23–40)	22 (21–30)	34 (31–48)†	20 (13–24)‡
HCO_3^-, mmol/L	13.0 (11.3–14.0)	13.2 (9.9–15.1)	12.5 (11.0–14.5)	9.1 (4.9–11.4)
Lactates, mmol/L	2.5 (2.3–2.7)	2.6 (2.5–3.0)	2.8 (2.4–3.0)	3.2 (2.7–4.1)
Bronchoalveolar lavage				
Cell count, cell/μl§	380 (105–845)	1,080 (535–1225)	2,255 (2005–2815)*,†	2,430 (2,047–2,800)*,†
Protein concentration, μg/ml	88 (22–145)	63 (18–185)	134 (120–233)*	250 (150–470)*,†
Lung histology				
Lung edema, % surface	45 (43–47)	43 (41–48)	50 (46–52)†	49 (46–50)*,†
Vascular congestion, % surface	75 (73–76)	74 (73–75)	79 (77–80) *,†	79 (77–80)*,†

Definition of abbreviations: DI, deep inflations; Pa_{CO_2}, arterial carbon dioxide tension; PaO_2/FI_{O_2}, ratio of arterial oxygen tension and fraction of inspired oxygen fraction; TI, tidal inflations.

Data are median (25th–75th percentile); $n = 7$–13 animals/group.

* P value < 0.05 (Mann-Withney test after Kruskal Wallis test) as compared to PBS + TI.

† P value < 0.05 (Mann-Withney test after Kruskal Wallis test) as compared to PBS + DI.

‡ P value < 0.05 (Mann-Withney test after Kruskal Wallis test) as compared to LPS + TI.

§ Differential cell count was performed in a limited number of animals and showed a predominance of polymorphonuclear neutrophils (>80% of total cells) in all groups.

TABLE 2. HEMODYNAMIC DATA AT THE END OF FIVE HOURS OF MECHANICAL VENTILATION USING TIDAL INFLATIONS OR DEEP INFLATIONS IN MICE THAT UNDERWENT PBS OR LPS ASPIRATION

	PBS + TI	PBS + DI	LPS + TI	LPS + DI
Heart rate, bpm	540 (535–570)	530 (503–563)	550 (500–580)	530 (515–573)
Right ventricular systolic pressure, mm Hg	27 (24–29)	35 (31–40)*	37 (35–38)*	49 (46–54)*,†,‡
Cardiac output, ml/min	23 (21–30)	19 (18–31)	25 (18–29)	22 (17–26)
Total pulmonary resistance, mm Hg · min/ml	1.06 (0.90–1.36)	1.84 (1.25–2.09)*	1.48 (1.24–1.97)*	2.43 (2.32–2.51)*,†,‡

Definition of abbreviations: DI, deep inflations; TI, tidal inflations.
Data are median (25th–75th percentile); $n = 9$ to 13 animals per group.
* P value < 0.05 (Mann-Withney test after Kruskal Wallis test) as compared to PBS + TI.
† P value < 0.05 (Mann-Withney test after Kruskal Wallis test) as compared to PBS + DI.
‡ P value < 0.05 (Mann-Withney test after Kruskal Wallis test) as compared to LPS + TI.

were validated by quantitative RT-PCR (Figure 5B). In addition, the angiopoietin-2:angiopoietin-1 gene expression ratio, a metric for vascular dysfunction, was significantly increased only in the LPS + DI group (Figure 5C) when compared with the PBS + TI group.

Similar to lung expression profiles, right ventricle gene expression analysis showed differential expression in both LPS + TI and LPS + DI mice, whereas PBS + DI had no significant impact. Gene ontology and pathway functional annotation clustering revealed little overlap between dysregulated terms in right ventricles from LPS + TI and LPS + DI groups, with only two common enriched clusters among the top 10 (extracellular matrix and platelet-derived growth factor binding). Clusters enriched by genes dysregulated in right ventricles from LPS + DI animals, but not enriched by LPS + TI, involved the acute inflammatory response, apoptosis, and membrane organization (Figure E3). Unlike lung and right ventricle gene expression, left ventricle gene expression profiling displayed significant dysregulation in PBS + DI–exposed mice as well as LPS + TI and LPS + DI animals, with three top-10 enriched gene ontology and pathway clusters shared by PBS + DI– and LPS + TI–challenged mice (mitochondria/cellular respiration, nucleotide binding, and contractile apparatus) (Figure E4).

Effect of DI on Indices of Lung and Systemic Inflammation

Predictably, BAL concentrations for the vast majority of cytokines/chemokines assayed (25 out of 27) were significantly increased in LPS-challenged mice (as compared with PBS + TI), with equivalent fold changes observed in LPS + TI and LPS + DI mice (Figure 6A). The concentrations of 10 out of 27 cytokines/chemokines, as well as all four endothelial markers assayed in plasma, were significantly increased in LPS-challenged mice (compared with PBS + TI). For these 14 differentially

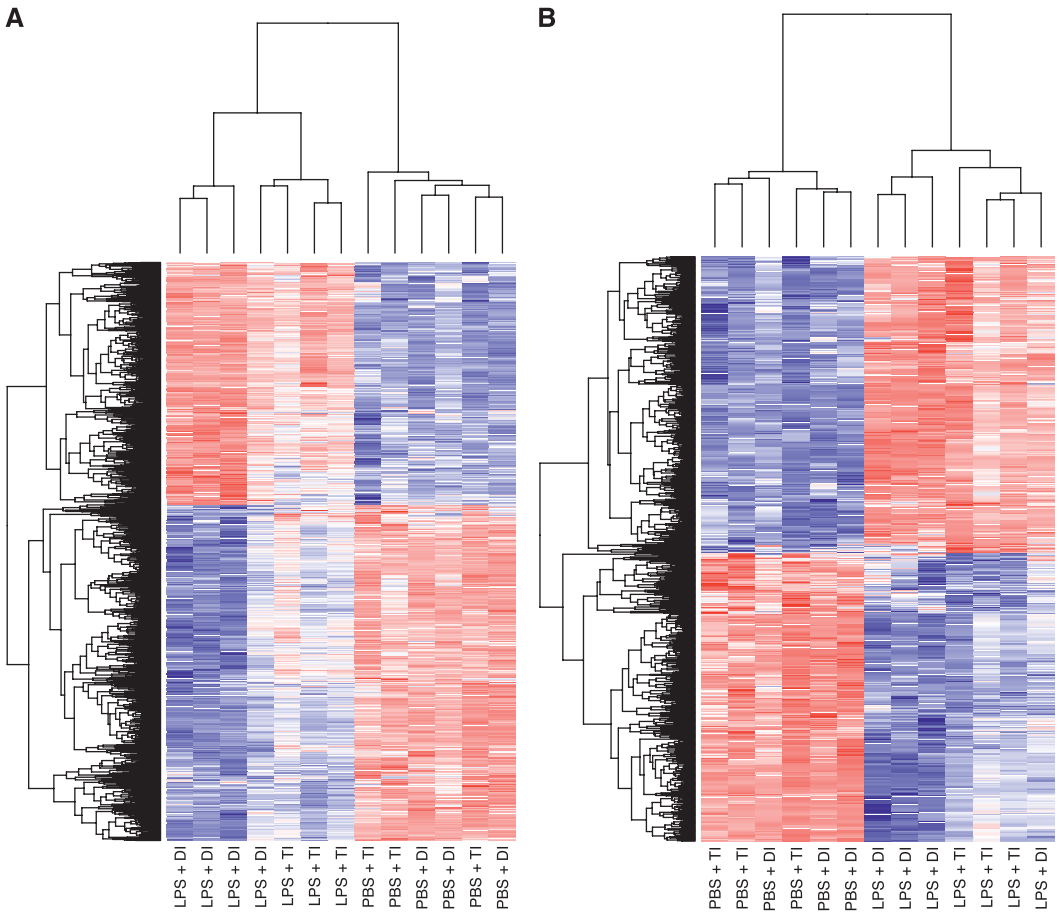

Figure 3. Expression pattern of dysregulated lung genes in mice exposed to mechanical ventilation using TIs or DIs after PBS or LPS aspiration. The expression levels of dysregulated lung genes identified using significance analysis of microarrays for LPS + DI versus PBS + TI comparison (*A*) and for LPS + TI versus PBS + TI comparison (*B*) are displayed by hierarchical clustering (using Bioconductor). Sample clustering is displayed at the *top*; gene clusters are displayed on the *left*; *blue*, *white*, and *red* represent expression levels below, at, and above mean level, respectively.

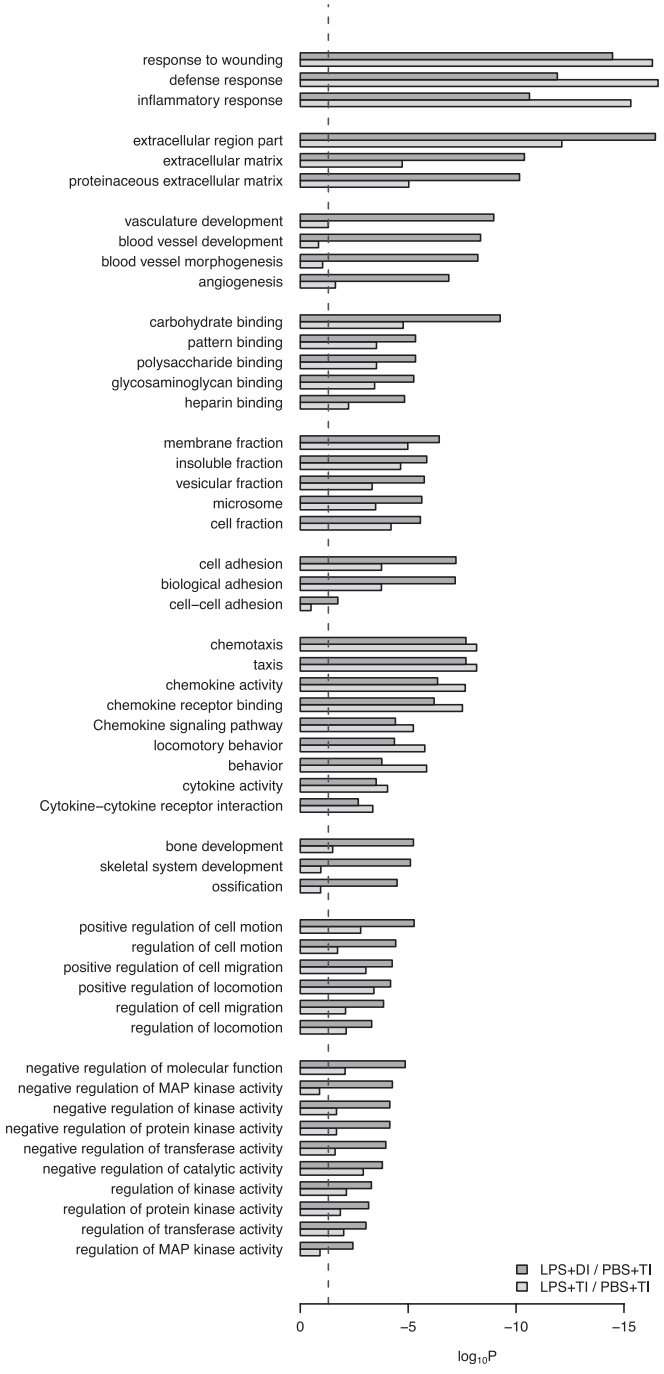

Figure 4. Top 10 clusters of gene ontology categories and pathways enriched by genes dysregulated by LPS + DI (using PBS + TI as the reference group) in lungs. Groups were compared using significance analysis of microarray (LPS + DI versus PBS + TI and LPS + TI versus PBS + TI), and the lists of dysregulated genes were explored by Database for Annotation, Visualization and Integrated Discovery functional annotation clustering to assess significance of gene-term enrichment. *Bars* represent the log-transformed enrichment *P* value (modified Fischer's exact test) of each category for the LPS + DI versus PBS + TI comparison (*dark gray*) and for the LPS + TI versus PBS + TI comparison (*light gray*). The top 10 clusters are those with the highest enrichment score (calculated as the geometric mean of the enrichment *P* values of all categories within the cluster) for the LPS + DI versus PBS + TI comparison. The *vertical dashed line* represents the 0.05 significance threshold. TI, ventilation with TIs only.

expressed proteins, equivalent fold changes were observed in LPS + TI and LPS + DI for 11 proteins, with significantly higher fold changes with LPS + DI as compared with LPS + TI for leukemia inhibitory factor, IL-6, and total plasminogen activator inhibitor-1 levels (Figure 6B).

DISCUSSION

In the setting of modest positive end-expiratory pressure (PEEP) and low tidal volume ventilation, we examined the effects of prolonged ventilation with intermittent DI delivery on lung mechanics, right ventricle hemodynamics, and cardiopulmonary gene expression in mice with or without prior lung injury. DI maneuvers significantly alleviated lung mechanic alterations produced by low tidal volume ventilation. However, these benefits were accompanied by increases in right ventricle pressures and total pulmonary vascular resistances, especially in the setting of LPS-induced lung injury. Genome-wide expression profiling provided compelling corroborative evidence that DI strategies produce vascular dysfunction and sustained inflammation in LPS-challenged lungs.

After LPS aspiration, mice exhibited higher values of dynamic elastance, tissue damping, and tissue elastance as compared with those having received PBS, and this difference partially persisted after volume history standardization and during mechanical ventilation. The alteration of mechanical properties of the lung after LPS aspiration is in line with previous reports (29) and consistent with the inflammatory changes eventually observed in tissues (gene expression by microarray) and BAL fluid (cell count and cytokine concentrations). Consistent with its potential to prevent alveolar derecruitment, DI resulted in more effective ventilation, as shown by the trend toward lower Pa_{CO_2} values in animals receiving DI, despite all groups being matched to the same total minute ventilation. Mechanical ventilation with TI was associated with a dramatic impairment in resistive and elastic properties of lung tissue in both PBS- and LPS-challenged mice, which were significantly mitigated by the use of DI. In particular, DI reduced the striking increase in tissue damping and tissue elastance observed with TI ventilation. These findings are in line with previous reports highlighting a progressive alteration of lung mechanics during low tidal volume ventilation in mice, which can be attributed to atelectasis and prevented by DI (8).

Despite their beneficial effect on lung mechanics, DI maneuvers were associated with significant increases in right ventricle systolic pressure and total pulmonary vascular resistances, especially in LPS-challenged animals. We interpret these findings to be in accordance with previous experimental and clinical studies showing an increase in right ventricle afterload during recruitment maneuvers (10–13, 30). Although a normal right ventricle (RV) could not theoretically generate very high pressures in an acute setting, the time constant of RV adaptation to increased afterload is not well known, and mild RV hypertrophy has been described after several hours of hypoxemic respiratory failure in patients free of any underlying pathological conditions (31). We attempted to determine molecular signatures that describe the effects of LPS-induced lung injury and those of mechanical ventilation with DI by performing extensive expression profiling of lung and cardiac tissues. Interestingly, a cluster involving the lung vasculature was enriched in genes dysregulated by LPS + DI, but not in those dysregulated by LPS + TI, highlighting the potential involvement of lung vascular dysfunction in the rise in right ventricle pressures observed in LPS + DI mice. Several genes implicated in endothelial injury, vascular tone, vascular remodeling, and microvascular thrombosis were highly dysregulated in LPS + DI lungs. Of note, the ratio of angiopioetin-2 to angiopoietin-1 gene expression was significantly increased in the LPS + DI group as compared

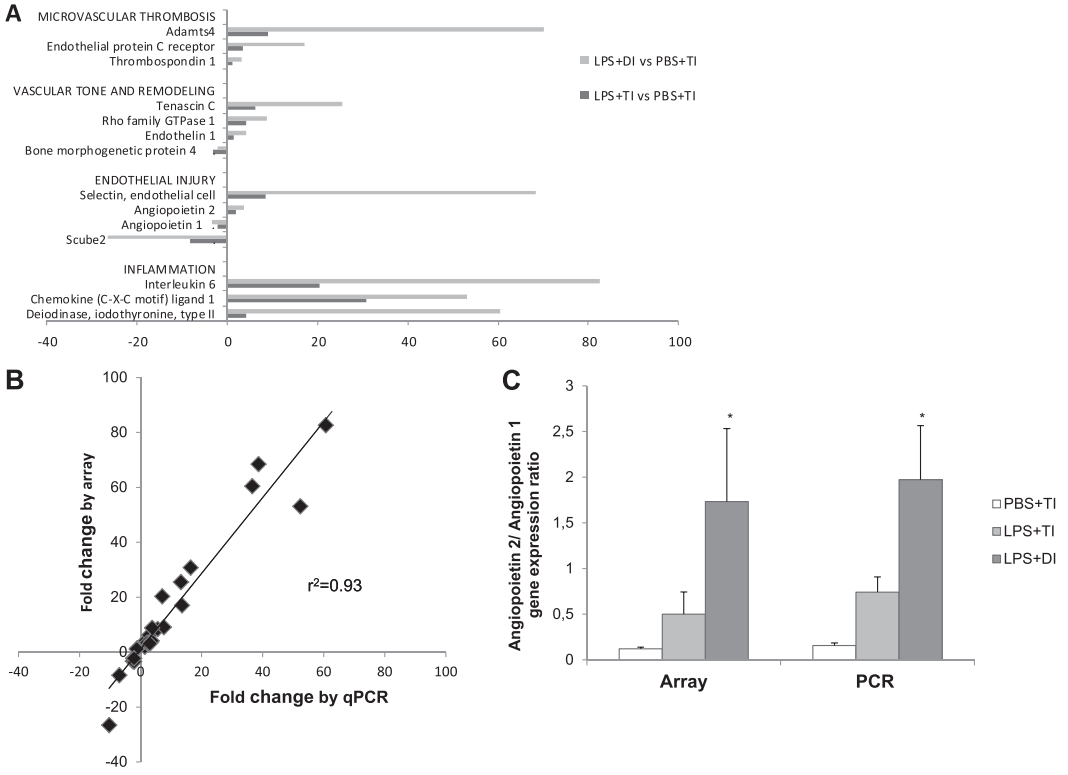

Figure 5. Fold changes in lung microarray expression of selected genes involved in inflammation and vascular dysfunction. Comparisons of gene expression after LPS + DI versus PBS + TI (*light gray*) and LPS + TI versus PBS + TI (*dark gray*) (*A*) and their correlation with RT-PCR validation assays (*B*). (*C*) The ratio of angiopoietin-2 to angiopoietin-1 array expression level (mean and SEM) in each group. LPS, LPS aspiration; qPCR, quantitative PCR; TI, ventilation with TIs only; Scube2, signal peptide CUB domain epidermal growth factor–like 2.

with PBS + TI. Angiopoietin-1 and -2 are vascular growth factors that classically act in an agonist/antagonist manner on the endothelial tyrosine kinase receptor to influence integrity and function of the vascular endothelium, particularly with regard to lung vascular permeability (32). The ratio of angiopioetin-2 to -1 plasma concentrations has been recently proposed as a marker of endothelial injury and validated as a predictor of mortality in patients with ALI (33).

Our findings of deleterious effects of DI on pulmonary vascular and right ventricular function may seem in contradiction to a previous report by Duggan and colleagues (34) that recruitment maneuvers reversed vascular leak and right ventricular failure caused by atelectasis. Several differences between the two studies may explain the dissimilar results (34). First, this study used a model of uninjured rat lungs ventilated for a shorter period (2.5 h), a strategy that may minimize lesions associated with the repetition of overdistention and vascular stretch with DI. Our studies used a murine model of lung injury with prolonged ventilation (5 h) to mimic the human condition where patients with ALI/ARDS exhibit significant lung injury and are typically ventilated for several days. During prolonged ventilation, the benefits of recruitment may be outweighed by cumulative damage from excessive overdistention. High tidal volume ventilation, which is an extreme case of delivering DI with every breath, has been known for several decades to be injurious to the lung (35–37). Our study suggests that frequency of high tidal ventilation required to induce vascular injury is much lower than might previously have been thought. A second difference in these two studies is the ventilation of the rat control group with zero PEEP (a strategy known to be injurious because of cyclic opening and closing of pulmonary units), whereas our murine studies used moderate PEEP (3 cm H_2O) in all groups. A third key difference is the nature of strategies used for recruitment of atelectatic lung. Clearly, a variety of strategies may accomplish this, including application of high PEEP (38, 39). For lung recruitment, the rat studies applied 2 cm H_2O PEEP throughout the ventilatory protocol, with intermittent increases to 8 cm H_2O, whereas we employed DI. Whether the use of such PEEP levels in our model would have effects that differed from those of DI warrants further examination.

This is the first study to explore right and left heart gene expression in a model of ALI. We identified ontology clusters enriched by right ventricle genes dysregulated in LPS + DI animals, but not enriched by LPS + TI that involved genes associated with acute inflammatory responses, apoptosis, and membrane organization. Given that the LPS + DI group exhibited the highest values of right ventricle systolic pressures, these three pathways are likely involved in the cardiac transcriptional response to acute pulmonary hypertension. Consistent with this notion, a recent study assessing right ventricle gene expression in a rat model of pulmonary embolism with pulmonary hypertension found a robust inflammatory response within the right ventricle tissue (40). In our study, transcriptional changes in the left ventricle shared four major gene ontology clusters that involved the mitochondrion/cellular respiration, ATP binding, catabolic processes, and sarcomere, findings very similar to the transcriptional changes in energy metabolism and contractile-related genes identified as key elements of sepsis-induced myocardial depression (41).

Although extrapolation of experimental findings to the human condition should obviously be undertaken with significant caution, our study provides several potentially important clinical implications. First, our results may discourage the systematic use of frequent lung recruitment maneuvers during prolonged ventilation, although the range of volumes used for DIs in our experimental model, as well as murine chest wall properties, are very different from the clinical scenario. Lung recruitment maneuvers have been proposed for use during anesthesia and after surgery for atelectasis prevention, as well as in patients with ARDS to reverse lung atelectasis. To date, these maneuvers have not been proven to significantly decrease overall morbidity or mortality (42). Second, our data also clearly display an existing discrepancy between

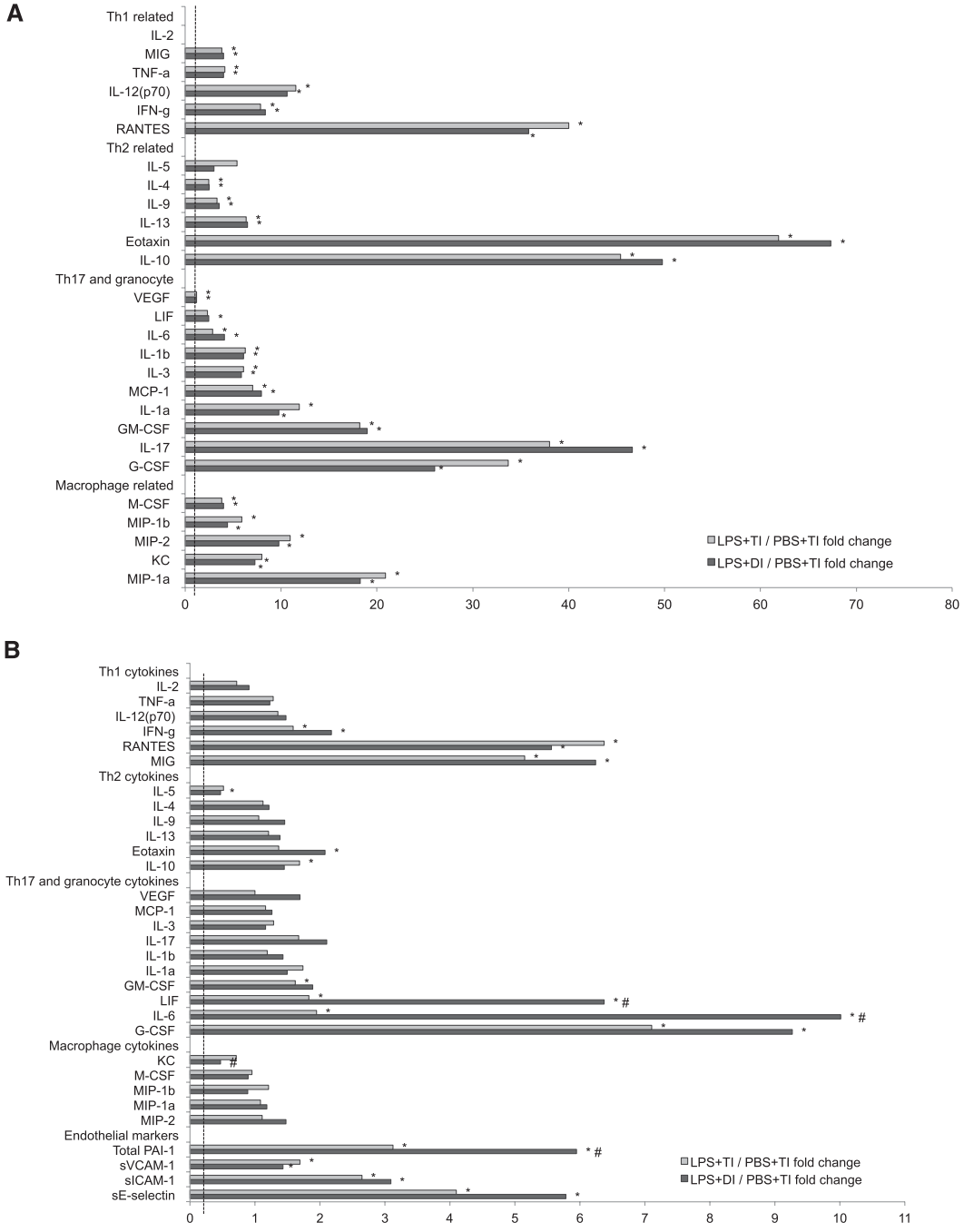

Figure 6. Fold changes in concentrations of various cytokines, chemokines, and endothelium markers in bronchoalveolar lavage (*A*) and plasma (*B*) by multianalyte assay for LPS + DI versus PBS + TI (*dark gray*) and LPS + TI versus PBS + TI (*light gray*) comparisons. $^{*}P < 0.05$ (Mann-Withney test after Kruskal-Wallis test) as compared with PBS + TI; $^{\#}P < 0.05$ (Mann-Whitney test after Kruskal-Wallis test) as compared with LPS + TI. G-CSF, granulocyte colony-stimulating factor; GM-CSF, granulocyte/macrophage colony–stimulating factor; KC, keratinocyte-derived cytokine; LIF, leukemia inhibitory factor; M-CSF, macrophage colony-stimulating factor; MCP, monocyte chemoattractant protein; MIG, monokine induced by interferon-γ; MIP, macrophage inflammatory protein; PAI, plasminogen activator inhibitor; RANTES, regulated upon activation, normal T cell expressed and secreted; sICAM, soluble intercellular adhesion molecule; sVCAM, soluble vascular cell adhesion molecule; Th, T helper cell; VEGF, vascular endothelial growth factor.

physiological and biological lung responses in the context of ALI. In general, an intervention associated with improvement in lung mechanics is assumed to produce similar advantageous effects at the cellular level. Despite clearly beneficial effects on lung mechanics, DI did not reduce overall lung biotrauma in our model and, in fact, produced either similar or worsened gene expression dysregulation compared with LPS + TI–exposed mice. The increase in BAL and plasma concentration of various cytokines, chemokines, and endothelial markers was either similar in these two groups or more aberrant in LPS + DI–challenged animals, as was the case for leukemia inhibitory factor, IL-6, and total plasminogen activator inhibitor-1. Our findings suggest the utility of assessing both physiological and biological markers to accurately interpret the impact of ventilator settings in the clinical scenario. These results also demonstrate the experimental occurrence of pulmonary vascular dysfunction, even in the context of reduced airway pressures and improved lung mechanics. It has been reported for several years that, besides the epithelial injury, ARDS is also a disease of the pulmonary circulation (43) that can affect the right ventricle (44), highlighting the need for an optimal balance between hemodynamics and respiratory mechanics. A recent study reported that pulmonary vascular dysfunction (defined as an increase in transpulmonary gradient or pulmonary vascular resistance) is common in ALI and independently associated with poor outcomes (15). In the Respiratory Management of Acute lung Injury Study of the ARDSNetwork (2), patients had a better outcome when using a low tidal volume, despite significantly worse oxygenation, illustrating the risks of looking at a single physiological endpoint of respiratory function. Our study provides a dramatic example of improvement in lung mechanical properties being associated with a significant worsening of vascular function and inflammation.

In conclusion, we observed a striking deterioration of lung mechanics in mice subjected to prolonged low tidal volume ventilation after PBS or LPS aspiration. This deterioration was remarkably mitigated by DI recruitment maneuvers. However, in LPS-challenged animals, DI did not attenuate lung inflammatory transcriptional profile, but rather produced dysregulation of several vascular genes, resulting in an increase in right ventricle afterload. Gene ontology identified inflammation, apoptosis, and membrane organization as potential key elements of the right ventricle response to acute pressure overload, whereas the left ventricle transcriptional profile often revealed dysregulated genes in energy metabolism, nucleotide binding, and contractile apparatus.

Author disclosures are available with the text of this article at www.atsjournals.org.

Acknowledgments: The authors are very grateful to the following members of the University of Illinois at Chicago's Institute for Personalized Respiratory Medicine for their invaluable help: Biji Mathew, Ph.D., Jessica Siegler, XiaoGuang Sun, M.D., Ph.D., Michael Wade, and Eddie Chiang. They are also indebted to Shwu-Fan Ma, Ph.D. (Section of Pulmonary and Critical Care, University of Chicago), Ryan Deaton (Department of Pathology, University of Illinois at Chicago), as well as Rachid Souktani, Ph.D. (Plateforme Petit Animal, INSERM U955, Créteil), for invaluable scientific and technical assistance.

References

1. Amato MB, Barbas CS, Medeiros DM, Magaldi RB, Schettino GP, Lorenzi-Filho G, Kairalla RA, Deheinzelin D, Munoz C, Oliveira R, *et al*. Effect of a protective-ventilation strategy on mortality in the acute respiratory distress syndrome. *N Engl J Med* 1998;338: 347–354.
2. Ventilation with lower tidal volumes as compared with traditional tidal volumes for acute lung injury and the acute respiratory distress syndrome. The Acute Respiratory Distress Syndrome Network. *N Engl J Med* 2000;342:1301–1308.
3. Esteban A, Ferguson ND, Meade MO, Frutos-Vivar F, Apezteguia C, Brochard L, Raymondos K, Nin N, Hurtado J, Tomicic V, *et al*. Evolution of mechanical ventilation in response to clinical research. *Am J Respir Crit Care Med* 2008;177:170–177.
4. Richard JC, Maggiore SM, Jonson B, Mancebo J, Lemaire F, Brochard L. Influence of tidal volume on alveolar recruitment: respective role of PEEP and a recruitment maneuver. *Am J Respir Crit Care Med* 2001;163:1609–1613.
5. Carpenter TC, Stenmark KR. Hypoxia decreases lung neprilysin expression and increases pulmonary vascular leak. *Am J Physiol Lung Cell Mol Physiol* 2001;281:L941–L948.
6. Madjdpour C, Jewell UR, Kneller S, Ziegler U, Schwendener R, Booy C, Klausli L, Pasch T, Schimmer RC, Beck-Schimmer B. Decreased alveolar oxygen induces lung inflammation. *Am J Physiol Lung Cell Mol Physiol* 2003;284:L360–L367.
7. Muscedere JG, Mullen JB, Gan K, Slutsky AS. Tidal ventilation at low airway pressures can augment lung injury. *Am J Respir Crit Care Med* 1994;149:1327–1334.
8. Allen GB, Suratt BT, Rinaldi L, Petty JM, Bates JH. Choosing the frequency of deep inflation in mice: balancing recruitment against ventilator-induced lung injury. *Am J Physiol Lung Cell Mol Physiol* 2006;291:L710–L717.
9. Grasso S, Mascia L, Del Turco M, Malacarne P, Giunta F, Brochard L, Slutsky AS, Marco Ranieri V. Effects of recruiting maneuvers in patients with acute respiratory distress syndrome ventilated with protective ventilatory strategy. *Anesthesiology* 2002;96:795–802.
10. Fujino Y, Goddon S, Dolhnikoff M, Hess D, Amato MB, Kacmarek RM. Repetitive high-pressure recruitment maneuvers required to maximally recruit lung in a sheep model of acute respiratory distress syndrome. *Crit Care Med* 2001;29:1579–1586.
11. Lim SC, Adams AB, Simonson DA, Dries DJ, Broccard AF, Hotchkiss JR, Marini JJ. Transient hemodynamic effects of recruitment maneuvers in three experimental models of acute lung injury. *Crit Care Med* 2004;32:2378–2384.
12. Odenstedt H, Aneman A, Karason S, Stenqvist O, Lundin S. Acute hemodynamic changes during lung recruitment in lavage and endotoxin-induced ali. *Intensive Care Med* 2005;31:112–120.
13. Nielsen J, Nilsson M, Freden F, Hultman J, Alstrom U, Kjaergaard J, Hedenstierna G, Larsson A. Central hemodynamics during lung recruitment maneuvers at hypovolemia, normovolemia and hypervolemia: a study by echocardiography and continuous pulmonary artery flow measurements in lung-injured pigs. *Intensive Care Med* 2006;32:585–594.
14. Mekontso Dessap A, Charron C, Devaquet J, Aboab J, Jardin F, Brochard L, Vieillard-Baron A. Impact of acute hypercapnia and augmented positive end-expiratory pressure on right ventricle function in severe acute respiratory distress syndrome. *Intensive Care Med* 2009;35:1850–1858.
15. Bull TM, Clark B, McFann K, Moss M. Pulmonary vascular dysfunction is associated with poor outcomes in patients with acute lung injury. *Am J Respir Crit Care Med* 2010;182:1123–1128.
16. Mekontso Dessap AVG, Zhou T, Marcos E, Dudek SM, Jacobson JR, Machado R, Adnot S, Brochard L, Maitre B, Garcia JGN. Cardiopulmonary effects of recruitment maneuvers in murine acute lung injury highlight conflicting physiological and genomic indices [abstract]. *Am J Respir Crit Care Med* 2011;183:A4004.
17. Foster WM, Walters DM, Longphre M, Macri K, Miller LM. Methodology for the measurement of mucociliary function in the mouse by scintigraphy. *J Appl Physiol* 2001;90:1111–1117.
18. Thammanomai A, Majumdar A, Bartolak-Suki E, Suki B. Effects of reduced tidal volume ventilation on pulmonary function in mice before and after acute lung injury. *J Appl Physiol* 2007;103:1551–1559.
19. Pillow JJ, Korfhagen TR, Ikegami M, Sly PD. Overexpression of tgf-alpha increases lung tissue hysteresivity in transgenic mice. *J Appl Physiol* 2001;91:2730–2734.
20. Hantos Z, Daroczy B, Suki B, Nagy S, Fredberg JJ. Input impedance and peripheral inhomogeneity of dog lungs. *J Appl Physiol* 1992;72:168–178.
21. Champion HC, Villnave DJ, Tower A, Kadowitz PJ, Hyman AL. A novel right-heart catheterization technique for *in vivo* measurement of vascular responses in lungs of intact mice. *Am J Physiol Heart Circ Physiol* 2000;278:H8–H15.
22. Gilbertson JR, Ho J, Anthony L, Jukic DM, Yagi Y, Parwani AV. Primary histologic diagnosis using automated whole slide imaging: a validation study. *BMC Clin Pathol* 2006;6:4.
23. Hong SB, Huang Y, Moreno-Vinasco L, Sammani S, Moitra J, Barnard JW, Ma SF, Mirzapoiazova T, Evenoski C, Reeves RR, *et al*. Essential role of pre–B-cell colony enhancing factor in ventilator-induced lung injury. *Am J Respir Crit Care Med* 2008;178:605–617.
24. Meyer NJ, Huang Y, Singleton PA, Sammani S, Moitra J, Evenoski CL, Husain AN, Mitra S, Moreno-Vinasco L, Jacobson JR, *et al*. GADD45a is a novel candidate gene in inflammatory lung injury via influences on Akt signaling. *FASEB J* 2009;23:1325–1337.
25. Li C, Hung Wong W. Model-based analysis of oligonucleotide arrays: model validation, design issues and standard error application. *Genome Biol* 2001;2:RESEARCH0032.
26. Bolstad BM, Irizarry RA, Astrand M, Speed TP. A comparison of normalization methods for high density oligonucleotide array data based on variance and bias. *Bioinformatics* 2003;19:185–193.
27. Tusher VG, Tibshirani R, Chu G. Significance analysis of microarrays applied to the ionizing radiation response. *Proc Natl Acad Sci USA* 2001;98:5116–5121.
28. Huang da W, Sherman BT, Lempicki RA. Systematic and integrative analysis of large gene lists using DAVID bioinformatics resources. *Nat Protoc* 2009;4:44–57.
29. Rocco PR, Momesso DP, Figueira RC, Ferreira HC, Cadete RA, Legora-Machado A, Koatz VL, Lima LM, Barreiro EJ, Zin WA. Therapeutic potential of a new phosphodiesterase inhibitor in acute lung injury. *Eur Respir J* 2003;22:20–27.
30. Nielsen J, Ostergaard M, Kjaergaard J, Tingleff J, Berthelsen PG, Nygard E, Larsson A. Lung recruitment maneuver depresses central hemodynamics in patients following cardiac surgery. *Intensive Care Med* 2005;31:1189–1194.
31. Jardin F, Dubourg O, Bourdarias JP. Echocardiographic pattern of acute cor pulmonale. *Chest* 1997;111:209–217.
32. Eklund L, Olsen BR. Tie receptors and their angiopoietin ligands are context-dependent regulators of vascular remodeling. *Exp Cell Res* 2006;312:630–641.
33. Ong T, McClintock DE, Kallet RH, Ware LB, Matthay MA, Liu KD. Ratio of angiopoietin-2 to angiopoietin-1 as a predictor of mortality in acute lung injury patients. *Crit Care Med* 2010;38:1845–1851.

34. Duggan M, McCaul CL, McNamara PJ, Engelberts D, Ackerley C, Kavanagh BP. Atelectasis causes vascular leak and lethal right ventricular failure in uninjured rat lungs. *Am J Respir Crit Care Med* 2003;167:1633–1640.
35. Dreyfuss D, Saumon G. Ventilator-induced lung injury: lessons from experimental studies. *Am J Respir Crit Care Med* 1998;157:294–323.
36. Slutsky AS. Lung injury caused by mechanical ventilation. *Chest* 1999; 116(1, Suppl)9S–15S.
37. Webb HH, Tierney DF. Experimental pulmonary edema due to intermittent positive pressure ventilation with high inflation pressures: protection by positive end-expiratory pressure. *Am Rev Respir Dis* 1974;110:556–565.
38. Gattinoni L, D'Andrea L, Pelosi P, Vitale G, Pesenti A, Fumagalli R. Regional effects and mechanism of positive end-expiratory pressure in early adult respiratory distress syndrome. *JAMA* 1993;269:2122–2127.
39. Halter JM, Steinberg JM, Schiller HJ, DaSilva M, Gatto LA, Landas S, Nieman GF. Positive end-expiratory pressure after a recruitment maneuver prevents both alveolar collapse and recruitment/derecruitment. *Am J Respir Crit Care Med* 2003;167:1620–1626.
40. Zagorski J, Sanapareddy N, Gellar MA, Kline JA, Watts JA. Transcriptional profile of right ventricular tissue during acute pulmonary embolism in rats. *Physiol Genomics* 2008;34:101–111.
41. dos Santos CC, Gattas DJ, Tsoporis JN, Smeding L, Kabir G, Masoom H, Akram A, Plotz F, Slutsky AS, Husain M, *et al*. Sepsis-induced myocardial depression is associated with transcriptional changes in energy metabolism and contractile related genes: a physiological and gene expression–based approach. *Crit Care Med* 2010;38:894–902.
42. Meade MO, Cook DJ, Guyatt GH, Slutsky AS, Arabi YM, Cooper DJ, Davies AR, Hand LE, Zhou Q, Thabane L, *et al*. Ventilation strategy using low tidal volumes, recruitment maneuvers, and high positive end-expiratory pressure for acute lung injury and acute respiratory distress syndrome: a randomized controlled trial. *JAMA* 2008;299: 637–645.
43. Zapol WM, Snider MT. Pulmonary hypertension in severe acute respiratory failure. *N Engl J Med* 1977;296:476–480.
44. Vieillard-Baron A, Schmitt JM, Augarde R, Fellahi JL, Prin S, Page B, Beauchet A, Jardin F. Acute cor pulmonale in acute respiratory distress syndrome submitted to protective ventilation: incidence, clinical implications, and prognosis. *Crit Care Med* 2001;29:1551–1555.